Improved Performance of Environmentally Friendly Blends of Biobased Polyethylene and Kraft Lignin Compatibilized by Reactive Extrusion with Dicumyl Peroxide

Sandra Rojas-Lema, Juan Ivorra-Martinez, Diego Lascano, Daniel Garcia-Garcia, and Rafael Balart**

In this work, different contents (0.25, 0.50, 0.75, and 1 phr) of dicumyl peroxide (DCP) are incorporated into the bio-based high-density polyethylene (bioPE)/kraft lignin (KL) blends with a composition of 80 and 20 wt%, respectively with the aim of improving overall performance. The samples are obtained by reactive extrusion and injection-molding process, and then their overall performance is assessed by tensile tests, thermal analysis, optical and surface appearance, and wettability studies. The obtained mechanical properties confirm the successful interaction between bioPE and KL due to the addition of organic peroxide, which plays a key role in compatibilization. In particular, bioPE/KL blends with 1 phr of DCP achieve an increase in elongation at break of about 300% together with a noticeable increase in the impact strength of about 29% higher than the uncompatibilized bioPE/KL blend, while the tensile modulus decreases 42%. In addition, images obtained by field emission scanning electron microscopy show that the presence of DCP in the blends enhances better dispersion of KL into the bioPE matrix. The wettability analysis indicates that KL and DCP affect the hydrophobicity of the neat bioPE. Therefore, the resultant blends can be considered as potential sustainable polymers with balanced properties.

1. Introduction

Lignin is an aromatic copolymer considered the second most abundant component of wood after cellulose.[1] It is constituted by three phenyl-propanols, namely, guaiacyl-propanol, syringyl-propanol, and *p*-hydroxy-phenyl propanol repeating units.[2,3] Lignin contains a large variety of functional groups, such as hydroxyls groups, carboxyl groups, which can form efficient H-bounding interactions.[4] In addition, lignin is considered the main renewable source of aromatic structures.[5] Different kinds of lignins, called technical lignins, are obtained after the delignification process, such as kraft lignin (KL), soda lignin, and organosolv lignin. KL, which is obtained from the kraft pulping process in the paper industry, accounts for the highest percentage in the lignin industry with approximately 85%.[2,6] Nevertheless only 2% of the KL is currently upgraded into high-value added products. The remaining KL is normally used in energy production, especially in the alkali recovery process, which indicates that this biopolymer is not properly valorized.[7,8] This lack of use of KL provides a great opportunity to develop new studies and possible applications. Currently, there are some areas in which KL has shown some promising results such as biochemicals after chemical pyrolysis or degradation,[7] as a heavy metal adsorbent,[9] as hydrogels,[10,11] and as filler,[12] among others.

The use of lignin as a polymer reinforcement has proven to be a good alternative due to its positive effects on the thermal and mechanical properties, oxidation delay, and thermal stability of lignin-based blends.[13–15] Some of the advantages of using lignin as reinforcement are its availability, low cost, biodegradable properties, environmentally friendly nature, and, its relative homogeneous distribution when blended with other materials.[16] Lignin has been considered a good filler to be used in polymeric matrices.[17] In some cases, lignin has been used to replace inorganic fillers, due to lignin is not abrasive and has low density.[18] Some of these studies include polypropylene (PP),[19,20] and polyvinyl alcohol (PVA)[21] as polymer matrices. Despite there are some studies related to polyethylene (PE) and lignin blends, the rise of bio-based PE (bioPE) gives an interesting opportunity to give high environmentally friendly polymer blends. BioPE, also known as "green PE", comes from bioethanol obtained in the processing of food crops such as

---

S. Rojas-Lema, J. Ivorra-Martinez, D. Lascano, D. Garcia-Garcia, R. Balart
Technological Institute of Materials (ITM)
Universitat Politècnica de València (UPV)
Alcoy 03801, Spain
E-mail: sanrole@epsa.upv.es; rbalart@mcm.upv.es

S. Rojas-Lema, D. Lascano
Escuela Politécnica Nacional
Quito 170517 Ecuador

The ORCID identification number(s) for the author(s) of this article can be found under https://doi.org/10.1002/mame.202100196

DOI: 10.1002/mame.202100196

sugarcane, maize, and wheat. BioPE is currently used due to its simplest chemical structure, and its wide commercial applications, being, therefore, an interesting alternative to petroleum-based PE.[22–25]

However, the incorporation of lignin in polymeric matrices causes some difficulties, due to their inherent differences in physical and chemical properties. One of the reasons is related to the polar nature of the phenolic and aliphatic –OH groups contained in the lignin structure, which causes incompatibility and low miscibility when blended with nonpolar synthetic polymers.[14] Therefore, some research works have focused on minimizing this drawback. For instance, some authors have focused their studies on a previous modification of lignin before it is blended with other nonpolar polymers.[18,26] Besides, another possibility is the use of reactive extrusion (REX) with organic peroxides such as dicumyl peroxide (DCP),[27] benzoyl peroxide,[28] or 2.5-dimethyl-2.5-di(tert-butylperoxy)hexane,[29] among others, which provide free radical formation in both lignin and base polymer, thus allowing somewhat improved interaction. On the other hand, the use of copolymers with dual functionality (polar-nonpolar) such as maleic anhydride grafted LDPE and PP,[30,31] PE grafted with glycidyl methacrylate (PE-g-GMA),[32] represent a technical solution, but the overall properties are not remarkably improved. REX is a simple technique that allows reaction between polymers during the extrusion process. The reaction is related to formation of free radicals. For this reason, organic peroxides are of particular interest in REX.

DCP is widely used as a cross-linking agent because peroxides activate the reaction between the polymer and functional chemical groups and form grafted and/or branched copolymers in the blend. According to Anbarasan et al.[33] DCP has shown higher efficiency in crosslinking HDPE, against other peroxides such as O,O-t-butyl O-2-ethylhexylperoxycarbonate, t-butyl peroxybenzoate, t-butyl 3,5,5-trimethylperoxyhexanoate, and t-butyl 2-ethylperoxyhexanoate. DCP must be used in low amounts so that it can contribute to the thermoplasticity of the material; otherwise, it could lead to gel formation and even more, to fully crosslinked structure.[29,34] Compatibilization by REX with DCP has been successfully used to improve the compatibility in physical blends with low miscibility, as is the case of poly(3-hydroxybutyrate) and poly(ε-caprolactone) blends,[35] ethylene-vinyl acetate copolymer (EVA-c) with virgin and recycled PE blends,[36] and, poly(lactide)/poly(butylene adipate-*co*-terephthalate) (PLA/PBAT) blends.[37] DCP has also been successfully used to improve polymer-fiber interactions in high-density PE-sisal fiber composites, with a typical DCP loading of 1 phr, showing its efficiency during REX of fiber-reinforced composites.[38] In addition, REX has been developed using other compatibilizers, for instance, Mei et al.[4] reported that interfacial interactions between lignin and ethylene-propylene-diene monomer (EPDM) could be improved with the use of maleic anhydride grafted PE-octene elastomer (POE-MA) as a reactive compatibilizer. Moreover, they reported the use of 3-amino-1,2,4-triazole (ATA) as POE-MA modifier to enhance improved reactivity. They concluded that the addition of 20 phr PEO-MA, 5 phr ATA, and 20–40 phr lignin to EPDM matrix gave the best-balanced properties. Huang et al.,[39] recently reported formation of coordination-based energy sacrificial bonds in the interface between lignin nanoparticles (LNP) and a polyolefin elastomer (POE) as rubber matrix to obtain high-performance thermoplastic elastomers.

Table 1. Summary of compositions according to the weight (wt%) and phr of bioPE with KL and DCP in different contents.

Sample	bioPE [wt%]	KL [wt%]	DCP [phr]
bioPE	100	–	–
bioPE/KL	80	20	–
bioPE/KL/0.25-DCP	80	20	0.25
bioPE/KL/0.50-DCP	80	20	0.50
bioPE/KL/0.75-DCP	80	20	0.75
bioPE/KL/1-DCP	80	20	1

Nevertheless, currently, there are no research works related to the use of DCP in REX compatibilization of renewable high-density PE and KL. For this reason, the aim of this study is to obtain environmentally friendly bio-based blends/composites by using bio-PE as a matrix, KL as filler, and DCP to enhance compatibilization by REX, since these materials have become an interesting alternative to substitute petroleum-based materials. To achieve this, different contents of DCP, namely 0.25, 0.50, 0.75, 1 weight parts of DCP per one hundred weight parts of the bioPE/KL blend (phr) were used in the REX process. The obtained samples from REX were further processed by injection-molding and characterized by tensile tests, thermal and thermomechanical analysis, morphological structure, optical appearance, and wettability studies.

2. Experimental Section

2.1. Materials

Bio-HDPE, SHA7260 grade, with a density of 0.955 g cm^{-3} was supplied in pellet form by FKuR Kunststoff GmbH (Willich, Germany) and manufactured by Braskem (São Paulo, Brazil). KL with low sulfonate content was supplied by Sigma-Aldrich S.A. (Madrid, Spain). DCP (98% purity) with a molecular weight of 270.37 g mol^{-1} was supplied by Sigma-Aldrich S.A. (Madrid, Spain).

2.2. Manufacturing of bioPE/KL Blends by REX

BioPE and KL were pre-homogenized in a zipper bag with DCP powder in different proportions as shown in **Table 1**. The amount of KL was set to a constant loading of 20 wt%. Kadla and Kubo[40] reported the study of blends between KL at different loadings (25, 50, 75, 87.5, 95, and 100 wt%) and poly(ethylene oxide) (PEO). They proved blends containing 25 wt% KL showed the highest elongation at break with a value of 19.7%, while other KL content in the blends was characterized by lower elongation at break values under 5%. On the other hand, Thakur et al.[41] reported a decrease in elongation at break in polybutylene succinate (PBS)-lignin blends above 30% lignin. Therefore, in this study, the KL content was set to 20 wt% and the effect of DCP loading was evaluated.

The materials were subjected to REX in a co-rotating twin-screw extruder from Construcciones Mecánicas Dupra, S.L., (Alicante, Spain). The screw diameter was 25 mm and the length-to-diameter ratio (L/D) was 24. During the melt processing, the temperature profile was set as follows: 153 °C (hopper) – 158 °C – 160 °C – 163 °C (die), whereas screw rotation speed was adjusted to 19 rpm to allow reactive compatibilization. The extruded strands were pelletized with an air-knife unit. The resultant pellets were dried at 60 °C for 72 h to remove moisture.

2.3. Characterization

2.3.1. Color Measurements

A colorimetric spectrophotometer Konica CM-3600d Colorflex-DIFF2, from Hunter Associates Laboratory, Inc. (Reston, VA, USA), was used to determine the color coordinates and color changes of the samples. Calibration of the instrument was performed with a white standard tile. The CIE Lab color space coordinates L^*, a^*, b^* were determined using the standard illuminant D65 and an observer angle of 10°. Coordinate L^* represents luminance, where $L^* = 0$ indicates dark and $L^* = 100$ stands for lightness, meanwhile color coordinates a^* and b^* represent color changes from red to green and from yellow to blue, respectively. The color difference ($\Delta E_{ab}{}^*$) was calculated using Equation (1):

$$\Delta E_{ab}{}^* = \sqrt{(\Delta L^*)^2 + (\Delta a^*)^2 + (\Delta b^*)^2} \tag{1}$$

where ΔL^*, Δa^*, and Δb^* represent the variations in the L^*, a^*, and b^* coordinates, respectively. The average values of at least five readings, were reported. The color changes on the samples were evaluated based on the $\Delta E_{ab}{}^*$. Values <1 means an unnoticeable color difference, values ranging between 1–2 indicate a slight color difference that can only be noticed by an experienced observer, values in the range of 2–3.5 indicate a noticeable difference by an inexperienced observer, values in the range of 3.5–5 indicate a noticeable difference and values above 5 indicate that different colors were noticeable.

2.3.2. Microscopy Characterization

The morphologies of the fractured surfaces of the injection-molded pieces after impact tests, were observed by field emission scanning electron microscopy (FESEM). A ZEISS ULTRA 55 FESEM microscope (Oxford Instruments, Abingdon, UK) was used at an acceleration voltage of 2 kV. Before the analysis, the samples were coated with a gold-palladium alloy in a sputter coater EMITECH mod. SC7620 Quorum Technologies Ltd., (East Sussex, UK).

2.3.3. Mechanical Tests

Tensile tests of the injection-molded pieces after REX were carried out at room temperature in a universal test machine Elib 50 from S.A.E. Ibertest (Madrid, Spain), following the guidelines of ISO 527-1:2012. A load cell of 5 kN and a cross-head speed of 5 mm min^{-1} was used during the tests. At least five different samples were tested for each composition and the corresponding parameters were averaged. Impact strength was carried out in a Charpy pendulum (1-J) on notched (0.25 mm radius V-notch) rectangular samples with dimensions of 80 × 10 mm^2, using a Metrotec S.A. (San Sebastián, Spain), following the guidelines of ISO 179-1:2010. Regarding hardness, a Shore D durometer 673-D from J. Bot S.A. Instrument (Barcelona, Spain) was used, according to ISO 868:2003 standard. Five different samples values were averaged.

2.3.4. Thermal Characterization

Samples were subjected to differential scanning calorimetry (DSC) analysis. The average weight used for each sample was comprised between 5–7 mg. The equipment used was a Mettler-Toledo 821 calorimeter (Schwerzenbach, Switzerland). Samples were placed in 40-µL aluminum-sealed crucibles, and the most relevant thermal parameters were obtained through a thermal cycle in three stages: initial heating from 30 to 160 °C, then cooling to −50 °C, and finally a second heating to 250 °C, at a heating/cooling rate of 10 °C min^{-1} in nitrogen atmosphere (with a constant flow rate of 66 mL min^{-1}). In the cooling stage, it was identified the crystallization temperature (T_c), while the melting temperature (T_m) and the melting enthalpy (ΔH_m) were collected from the second heating step. Additionally, crystallinity degree (X_c) was obtained, using Equation (2).

$$\mathrm{X_c} = \left[\frac{\Delta \mathrm{H_m}}{\Delta \mathrm{H^0_m} \times \mathrm{w}}\right] \times 100 \tag{2}$$

where, ΔH_m (J g^{-1}) corresponds to the melting enthalpy, ΔH^0_m (J g^{-1}) is the melting enthalpy for a theoretical 100% crystalline bioPE, with a value of 293 (J g^{-1}),[42] and w is the weight fraction of bioPE used in the sample.

The thermal stability of the different samples was analyzed by thermogravimetry (TGA) in a PT1000 from Linseis (Selb, Germany). Samples sizing 15–25 mg were first placed in standard 70-µL alumina crucibles and subjected to a heating program in a nitrogen atmosphere from 30 to 700 °C at a heating rate of 10 °C min^{-1}. The temperature measured for a mass loss of 5% ($T_{5\%}$) was considered as the onset degradation temperature, while the temperatures at the maximum were determined from the first derivative thermogravimetry curves (DTG). All the tests were performed in triplicate to ensure reproducibility.

2.3.5. Dynamic Mechanical Thermal Characterization

The dynamic mechanical thermal analysis (DMTA) was performed in a DMA-1 model from Mettler-Toledo S.A. (Barcelona, Spain), using a single cantilever setup. The injection-molded samples were subjected to a temperature sweep program from −150 to 120 °C at a heating rate of 2 °C min^{-1}. The selected frequency was 1 Hz with a force of 0.02 N. The maximum flexural deformation or cantilever deflection was set to 10 µm. Tests were made in triplicate.

2.3.6. Wettability

The static water-contact angle (θ) of bioPE and bioPE/KL blends with different percentages of DCP used in REX was obtained following the ISO 828:2013 standard, in an optical goniometer EasyDrop-FM140 from Kruss Equipment (Hamburg, Germany), and analyzed at room temperature. The liquid used for the analysis was distilled water with a volume of approximately 5 µL. All contact angles were measured at 7 s after the droplet was poured into the surface. At least, five different measurements for each film were obtained and averaged.

2.4. Statistical Analysis

The statistical analysis was carried out by evaluating the results at 95% confidence level ($p \leq 0.05$) by one-way analysis of variance following Tukey's test for the significant differences among the samples, using for this OriginPro 8 software (OriginLab Corporation, Northampton, MA, USA).

3. Results and Discussion

3.1. Optical Appearance and Morphological Properties of bioPE/KL Blends

In nature, lignin presentation is almost colorless. However, when it is converted by different processes to technical lignin such as KL, soda lignin, or organosolv lignin, its color changes to a dark one. This is due to the addition of some chromophores (quinone groups, conjugated double bonds, carbonyl groups, and free radicals) and auxochrome (phenolic hydroxyl groups, hydroxyl groups, and carboxyl groups) during the isolation processes.[13,43] In this context, the addition of the KL to the bioPE matrix causes a significative color variation regarding the neat bioPE sample, achieving a dark brown color. In other studies, similarities were observed.[32] This difference between the sample appearance is presented in **Figure 1**, while the surface color values obtained are gathered in **Table 2**. The importance to analyze the color variation in the blends is because it allows finding the possible similarity in appearance with other wood plastic composites (WPC), which raises the possibility to use them in different applications related. In particular, bioPE/KL compatibilized by REX with DCP, offers a dark brown color, it is possible to compare it with Eucalyptus gummifera, which is a species within the Eucalyptus family, that presents values of 37.36, 22.50, 23.35, for L^*, a^*, and b^*, respectively.[44] In this regard, bioPE/KL blends offered a similar lightness value to that of Eucalyptus gummifera, while values obtained for a^* and b^* show some slight variation, which indicates that the blends obtained in this study present low red and yellow appearance.

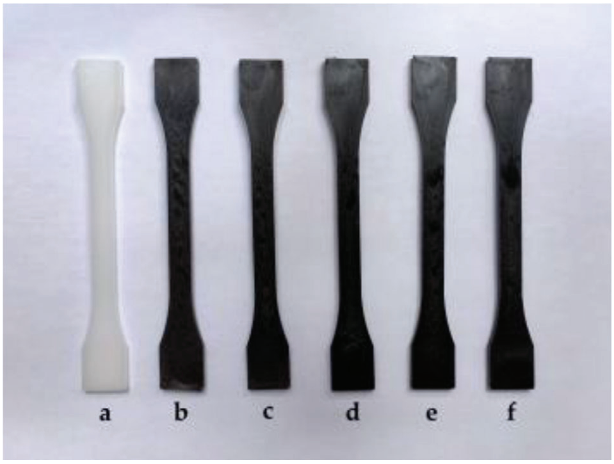

Figure 1. Injection-molded samples of bioPE/KL blends with different DCP amounts used in REX compatibilization: a) neat bioPE; b) bioPE/KL; c) bioPE/KL/0.25-DCP; d) bioPE/KL/0.50-DCP, e) bioPE/KL/0.75-DCP, and f) bioPE/KL/1-DCP.

Table 2. Color parameters (L^*, a^*, b^*) and color difference (ΔE_{ab}^*) of injection-molded samples of bioPE/KL blends with different DCP amounts used in the REX compatibilization.

Sample	L^*	a^*	b^*	ΔE_{ab}^*
bioPE	73.2 ± 0.9^{a}	-1.8 ± 0.6^{a}	-5.0 ± 0.1^{a}	–
bioPE/KL	32.3 ± 0.8^{b}	0.5 ± 0.0^{b}	1.1 ± 0.2^{b}	41.5 ± 0.8^{a}
bioPE/KL/0.25-DCP	32.3 ± 0.7^{b}	0.6 ± 0.0^{b}	1.7 ± 0.1^{c}	41.6 ± 0.7^{a}
bioPE/KL/0.50-DCP	32.1 ± 0.8^{b}	0.7 ± 0.1^{b}	2.1 ± 0.1^{d}	41.9 ± 0.7^{a}
bioPE/KL/0.75-DCP	30.7 ± 0.4^{c}	0.8 ± 0.1^{b}	$2.2 \pm 0.2^{d,e}$	43.2 ± 0.3^{b}
bioPE/KL/1-DCP	30.3 ± 0.3^{c}	0.7 ± 0.0^{b}	$1.9 \pm 0.2^{c,e}$	43.6 ± 0.3^{b}

$^{a\text{–}e}$Different letters in the same column indicate a significant difference among the samples ($p < 0.05$).

Figure 2 gathers the FESEM images of the fractured samples of neat bioPE, uncompatibilized bioPE/KL blend, and bioPE/KL blends subjected to REX with different DCP amounts. In Figure 2a it is possible to observe the fracture surface of neat bioPE, which shows high roughness and irregularities all over the surface. This is considered as a typical fracture surface of a ductile polymer, and it is in accordance with the work by Quiles-Carrillo et al.[45] Figure 2b shows the morphology of the uncompatibilized bioPE/KL blend. KL can be identified as the embedded phase with spherical and irregular shapes of KL. Similar findings were reported by Chen et al.[46] In addition, it is possible to identify some KL aggregates and holes over the surface, which indicate the poor compatibility between both biopolymers, since lignin particles tend to pull-out from the fractured surfaces.[22] This behavior is in total agreement with the study reported by He et al.[47] where content of LNP higher than 5 wt% shows also poor compatibility in a PVA matrix. One can also observe larger KL particles or aggregates since particles tend to interact with the same particles strongly due to the action of their hydrogen bonds and non-covalent π-π interaction between phenyl rings,[48] which cause coalescence and promote aggregation, especially when the amount of lignin used is high.[49] REX with DCP leads to some differences in morphology. In general, lignin aggregates are not observed which is representative for improved lignin dispersion into the bioPE matrix,[22] as it is can be seen in Figure 2c–f with increasing DCP in the REX process. It is important to remark that the dispersion state of the fillers in a polymer matrix could affect the polymer composites' performance.[46] Hence, if there is a good dispersion, it may improve the interaction between the bioPE and the KL. Furthermore, as observed in the FESEM

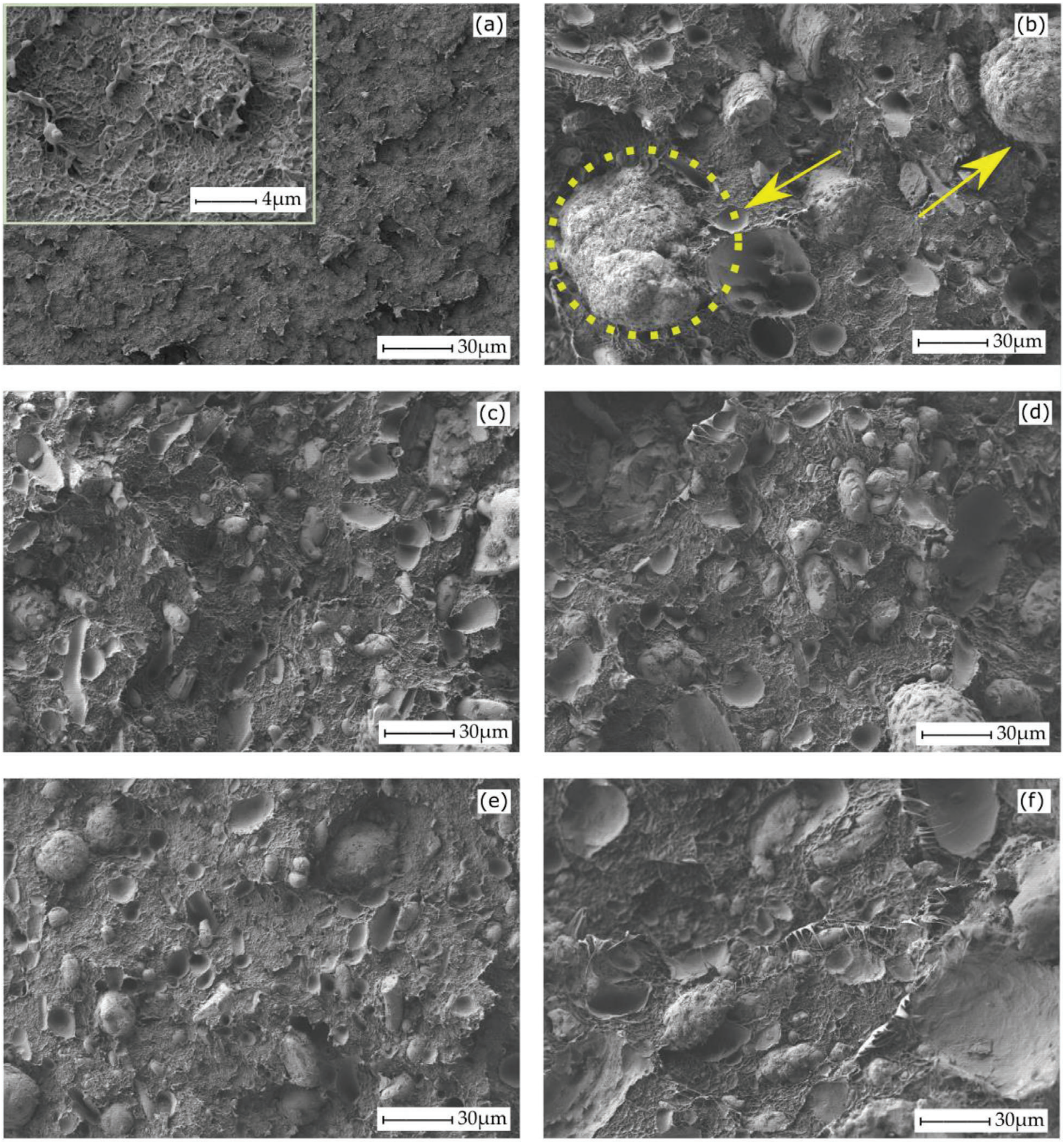

Figure 2. FESEM micrographs of the fractured surfaces of injection-molded samples of bioPE/KL blends with different DCP amounts used in REX compatibilization: a) neat bioPE, b) bioPE/KL, c) bioPE/KL/0.25-DCP, d) bioPE/KL/0.50-DCP, e) bioPE/KL/0.75-DCP, f) bioPE/KL/1-DCP. Images are taken at 500× with scale markers of 30 μm.

images of the REX-compatibilized blends, increasing the DCP content in the REX process, the aggregate disappears, thus indicating lignin domains are shorter and more homogeneous. This is best observed in the sample subjected to REX compatibilization with 1 phr DCP (Figure 2f). Therefore, it can be seen that REX with DCP is a technical solution to overcome the intrinsic immiscibility between the highly nonpolar bioPE matrix and the highly hydrophilic lignin polymer.

3.2. Mechanical Properties of bioPE/KL Blends

Table 3 gathers some of the mechanical properties of the uncompatibilized and REX-compatibilized bioPE/KL blends with increasing DCP content. As expected, neat bioPE is a very ductile polymer, with a tensile modulus of 778.4 MPa, a tensile strength of 18.2 MPa, and very high elongation at break (in fact it does not break in the used equipment). Similar tensile properties were

Table 3. Mechanical properties of the injection-molded samples of neat bioPE, uncompatibilized bioPE/KL blend and bioPE/KL blend compatibilized by REX with varying DCP content: tensile modulus (*E*), tensile strength at yield (σ_y), elongation at break (ϵ_b), impact energy, and Shore D hardness.

Sample	*E* [MPa]	σ_y [MPa]	ϵ_b [%]	Impact Energy[kJ m^{-2}]	Hardness[Shore D]
bioPE	778.4 ± 36.8 ^{a}	18.2 ± 0.7 ^{a}	NB	2.4 ± 0.1 ^{a}	58.2 ± 0.4 ^{a}
bioPE/KL	874.7 ± 76.1 ^{b}	15.8 ± 0.3 ^{b}	21.3 ± 1.7 ^{a}	1.5 ± 0.1 ^{b}	60.7 ± 1.0 ^{b}
bioPE/KL/0.25-DCP	564.2 ± 32.4 ^{b,c}	15.3 ± 0.4 ^{b,c}	23.0 ± 2.8 ^{a}	1.4 ± 0.0 ^{b}	60.8 ± 0.4 ^{b}
bioPE/KL/0.50-DCP	572.0 ± 35.7 ^{c}	15.1 ± 0.0 ^{c}	35.9 ± 1.6 ^{b}	1.5 ± 0.1 ^{b}	61.0 ± 0.0 ^{b}
bioPE/KL/0.75-DCP	545.1 ± 4.5 ^{b}	15.7 ± 0.1 ^{b}	63.1 ± 6.6 ^{c}	1.6 ± 0.3 ^{b,c}	61.0 ± 0.0 ^{b}
bioPE/KL/1-DCP	503.8 ± 32.9 ^{d}	16.8 ± 0.3 ^{d}	66.6 ± 6.0 ^{c}	1.9 ± 0.3 ^{c}	61.20 ± 0.4 ^{b}

$^{a–c}$ Different letters in the same column indicate a significant difference among the samples ($p < 0.05$).

reported by Espinach et al.[50] for neat bioPE. This is related to its T_g, that is commonly located below −100 °C.[51] Then, with the addition of KL into the bioPE matrix, an increase in the tensile modulus of about 12% and a decrease in the tensile strength of about 13%, respectively, were observed, which could be related to the aromatic and rigid structure of the lignin, and also due to its large interfacial area.[46] On the other hand, elongation at break is dramatically decreased down to values of 21.3%. Elongation at break is directly related to material's cohesion and poor interaction between the nonpolar bioPE and the polar KL, leads to poor stress transfer which, in turn, leads to a decrease in mechanical properties related to cohesion, such as elongation at break. This phenomenon leads to a more brittle blend.[45] A similar phenomenon was reported by Abdelwahab et al.[52] when lignin was added to PP matrix. Sameni et al.[53] also reported an increase in the tensile strength and tensile modulus in high-density PE (HDPE) reinforced with different loadings of soda lignin.

As can be observed in Table 3, after the REX process with increasing DCP, the tensile modulus of the compatibilized bioPE/KL blends decreases, being greater this decrement as DCP content increases in REX process. In this case, the lowest tensile modulus was obtained for the sample compatibilized by REX with 1 phr DCP, with a value of 503.8 MPa, which indicates a decrease close to 42% regarding the uncompatibilized bioPE/KL blend. Also, it can be seen REX with DCP hardly affected the tensile strength of the composites, which allowed to obtain very similar values of about 15 MPa. Only in the case of bioPE/KL blend subjected to REX with 1 phr DCP shows a slight increase in the tensile strength with a value of 16.8 MPa, which corresponds to an increase of the 6% regarding the bioPE/KL blend.

The most noticeable finding is that a remarkable improvement in the elongation at break is obtained in REX-compatibilized bioPE/KL blends with increasing DCP content. As can be observed in Table 3, with the increase of DCP during the REX compatibilization process, higher elongation at break was obtained, being the highest values 63.1% and 66.5% which correspond to REX with 0.75 phr DCP and 1 phr DCP, respectively, which indicates an increase nearly three times with regard to the uncompatibilized bioPE/KL blend. This improvement in the elongation at break could be related to the better dispersion and less tendency of KL to form aggregates as previously observed by FESEM analysis. Similar findings were reported by Ferri et al.[51] in immiscible poly(lactide)-poly(ethylene) blends by REX with DCP, which allowed a noticeable improvement in elongation at break in PLA/bioPE blends. On the other hand, the work by Fei et al.[54] indicated that the use of DCP as a crosslinking or reactive compatibilizer agent allowed to improve mechanical properties of poly [(3-hydroxybutyrate)-*co*-(3-hydroxyvalerate)] (PHBV); in particular, the elongation at break increased from 4% to 11%. Finally, Ma et al.[55] also observed as the incorporation of 0.5% of DCP allowed the increase of elongation at break from 8% to 400% in PHBV/PBS blends by reactive compatibilization.

Regarding the impact-absorbed energy, it can be observed that the incorporation of KL in the polymeric matrix of bioPE promotes a noticeable decrease in toughness compared to neat bioPE. This is due to the lack of interaction between these two materials, which causes stress concentration, generating, therefore, a brittle material, together with the aggregate formation phenomenon.[51] Neat bioPE presents an impact strength of 2.4 kJ m^{-2}, whilst the uncompatibilized bioPE/KL blends show a clear decrease down to 1.5 kJ m^{-2}, which represents a percentage decrease of 37%. As above-mentioned, some mechanical properties are particularly sensitive to material's cohesion and the impact strength is, together with the elongation at break, one of these properties, since the lack of interface interactions leads to poor load transfer and, subsequently, both the elongation at break and the impact strength decrease. Nevertheless, the effect of increasing DCP during the REX compatibilization process, is positive since it provides slightly increased impact strength values. REX compatibilization with 0.75 phr DCP and 1 phr DCP led to impact strength values of 1.6 and 1.9 kJ m^{-2}, which represent an increase of around 7% and 29% regarding the uncompatibilized bioPE/KL blend. Garcia-Garcia et al.[35] observed a similar tendency when using DCP as a reactive compatibilizer in binary poly (3-hydroxybutyrate) (P3HB) and poly (ε-caprolactone) (PCL) blends, obtaining a percentage increase in the impact-absorbed energy over 230% using 1 wt% of DCP during REX. Bova et al.,[34] reported a noticeable increase in the tensile strength of about 134% in blends of acrylonitrile-butadiene rubber (NBR)/softwood KL (SKL), by using DCP at 2.5 phr during reactive mixing. According to the obtained results, it is possible to say that REX compatibilization with DCP is an interesting approach to improve the interaction between bioPE and KL, with the subsequent positive effect on material's cohesion properties, such as elongation at break and impact strength that is remarkably improved with increasing DCP content during REX.

Finally, regarding Shore D hardness, Table 3 shows an increase in the hardness after blending with KL with values from 58.2 for neat bioPE to 60.7 for the uncompatibilized bioPE/KL blend. However, REX with different DCP loadings seems to have a very

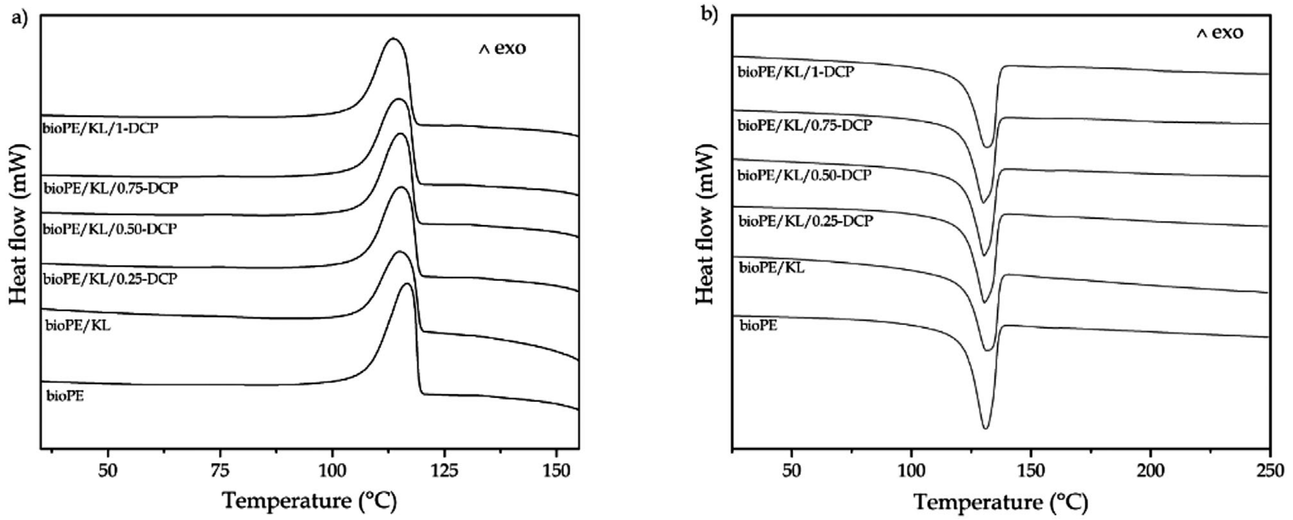

Figure 3. DSC thermograms of neat bioPE, uncompatibilized bioPE/KL blend and REX-compatibilized bioPE/KL blends with different DCP content, a) cooling and b) second heating cycle after the removal of the thermal history.

slight effect on hardness, since the Shore D hardness values for all bioPE/KL blends are close to 61. Therefore, it can be concluded that REX with DCP allows some compatibilization between bioPE and KL. REX compatibilization also prevents aggregate formation and this also has a positive effect on overall mechanical behavior of bioPE/KL blends. During REX, DCP recomposes at processing temperatures in the extruder and then, free radicals are formed in both bioPE and KL, thus allowing reaction between both polymers.[56,57]

3.3. Thermal Properties of bioPE/KL Blends

Figure 3 shows the DSC curves corresponding to the cooling step (Figure 3a) and second heating step (Figure 3b) once the thermal history has been removed. **Figure 4** shows the DSC characteristic curve of neat KL, in which, the glass transition temperature (T_g) can be clearly identified by the step of the base line at about 160 °C. Figure 3a shows bioPE crystallization peak during the cooling step. The crystallization temperature (T_c) for neat bioPE is close to was to 116.8 °C. The effect of REX with different DCP amounts is almost negligible since there is not a relevant change in the peak temperature (see **Table 4**). A slight decrease in T_c can be detected in REX-compatibilized bioPE/KL blends with 1 phr DCP. This decrease could be related to an increase in the molecular weight, branching, or reduction in chain mobility, which did not allow a good crystallization process when during cooling, causing some imperfect and small crystals and also in less quantity.[58] A similar tendency for crystallization was observed as shown in Zattera et al.[36] They revealed a decrease in T_c with increasing DCP in REX of LDPE-v/EVA. This effect was more pronounced since the amount of DCP used was over 1 phr. The melt peak of bioPE can be clearly seen in Figure 3b, located at about 130.9 °C and typical of an HDPE. This melt peak temperature (T_m) is almost the same for the uncompatibilized bioPE/KL blend. It is also worthy to note that REX with DCP does not affect the melt peak temperature with values close to 130 °C. Regard-

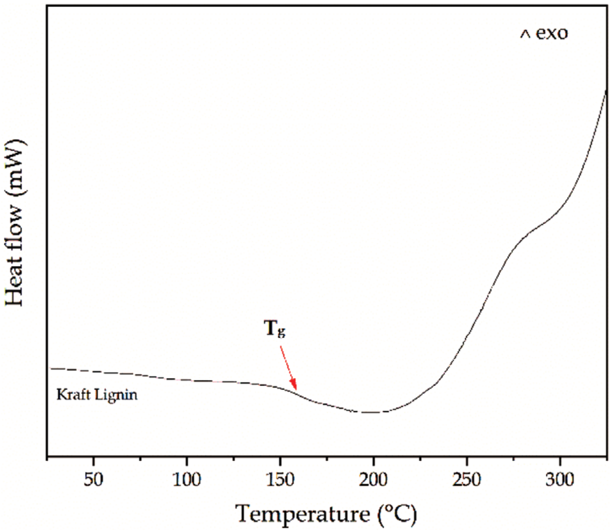

Figure 4. DSC thermogram of KL showing its glass transition temperature (T_g).

Table 4. Main thermal parameters of neat bioPE, uncompatibilized bioPE/KL blend and bioPE/KL blend compatibilized by REX with varying DCP content in terms of melting temperature (T_m), cooling temperature (T_c), normalized melting enthalpy (ΔH_m), and crystallinity degree (X_c).

Sample	T_c [°C]	T_m [°C]	ΔH_m [J g^{-1}]	X_c [%]
bioPE	116.8 ± 0.6^{a}	130.9 ± 0.9^{a}	185.4 ± 0.4^{a}	63.3 ± 0.2^{a}
bioPE/KL	115.5 ± 0.8^{a}	131.2 ± 0.5^{a}	150.2 ± 0.5^{b}	$64.1 \pm 0.4^{a,b}$
bioPE/KL/0.25-DCP	$115.4 \pm 0.5^{a,b}$	130.6 ± 0.4^{a}	$147.7 \pm 0.3^{b,c}$	$63.0 \pm 0.5^{a,c}$
bioPE/KL/0.50-DCP	115.3 ± 0.6^{b}	130.4 ± 0.4^{a}	$146.5 \pm 0.5^{c,d}$	62.5 ± 0.8^{a}
bioPE/KL/0.75-DCP	114.9 ± 0.9^{b}	130.1 ± 0.9^{a}	146.9 ± 0.8^{d}	62.6 ± 0.3^{c}
bioPE/KL/1-DCP	113.7 ± 0.5^{b}	131.2 ± 0.7^{a}	146.3 ± 0.4^{d}	62.4 ± 0.2^{c}

[a–d] Different letters in the same column indicate a significant difference among the samples ($p < 0.05$).

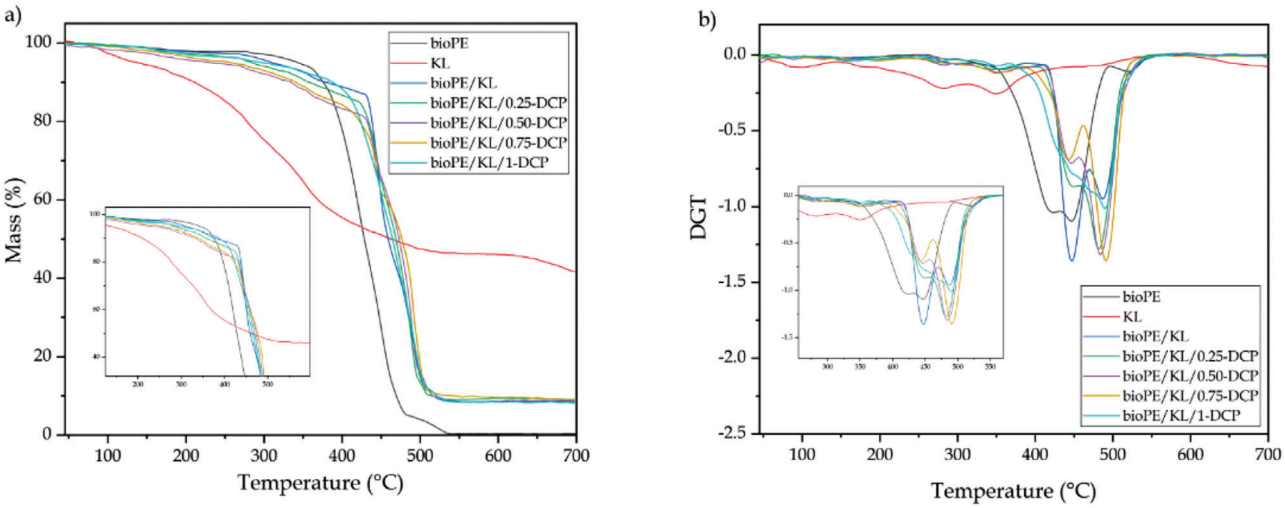

Figure 5. a) Thermogravimetric analysis (TGA) and b) first derivative (DTG) curves of the neat bioPE, uncompatibilized bioPE/KL blend and REX-compatibilized bioPE/KL blends with different DCP content.

ing the melt enthalpies, neat bioPE showed a normalized value of 185.4 J g^{-1}, while the uncompatibilized blend of bioPE with 20 wt% KL is close to 150.2 J g^{-1}, which is almost 19% lower than neat bioPE, due to the dilution effect. As slight decrease in the melt peak enthalpies can be detected in REX-compatibilized bioPE/KL blends with increasing DCP content. This could be related to less perfect crystals due to branches or crosslinked segments obtained during REX which, in turn, promote a slight decrease in crystallinity. A similar behavior was observed by Zattera et al.,[36] in LDPE-vEVA blends subjected to REX with DCP in the 1–4 phr. With regard to the degree of crystallinity, despite some tendency that could be assessed by seeing the values in Table 4, it is worthy to note that the crystallinity degree of neat bioPE is slightly increased for uncompatibilized bioPE/KL blends, while a slight decrease in crystallinity is detected in REX-compatibilized bioPE/KL blends as the DCP content increases, due to hindering provided by potential branching, crosslinking after reaction between both polymers (Table 4). This slight decrease in crystallinity provided by REX, agrees with the previous mechanical results since lower crystallinity leads to lower tensile modulus. This trend was also reported by Khonakdar et al.[58] in which, an increase of DCP in reactive compatibilization, causes a decrease in the melt peak temperature, crystallization temperature, and the degree of crystallinity. As above-mentioned, Figure 4 shows the DSC profile of neat KL, with an amorphous phase and a glass transition temperature (T_g) of 160.5 °C. It is worthy to remark that the T_g of KL can be affected by its molecular weight, thermal history, degree of crosslinking, and, polydispersity, among others.[53,59] Similar T_g values for lignin have been reported by Huang et al.,[59] with values of about 162 °C. The dilution effect does not allow clear observation of the T_g in DSC thermograms collected in Figure 4b. Nevertheless, in a qualitative way, a slight step in the baseline can be seen at about 160 °C in all bioPE/KL blends.

Figure 5 shows the thermogravimetric (TGA) curves for neat bioPE, uncompatibilized bioPE/KL blend, and REX-compatibilized bioPE/KL blend with increasing DCP loading. The thermal stability values obtained through TGA are summarized in **Table 5** with the onset degradation temperature ($T_{5\%}$), and the maximum degradation rates obtained by the first derivative of the TGA curve (1st DTG). Two main degradation peak values can be detected as a consequence of the reaction between both polymers in the REX process. It can be seen that neat KL shows lower thermal stability than neat bioPE. As one knows, lignin possesses a complex polymer structure that is progressively decomposed in a wide temperature range comprised between 200 and 500 °C. For this reason, the initial weight loss in lignin is higher than in bioPE that decomposes in a single step process. This initial weight loss in lignin could also be related to moisture due to its hydrophilicity.[60] Nevertheless, main degradation of lignin occurs between 200 and 500 °C, which is related to fragmentation of inter-unit linkages,[61] and corresponds to about 40% of the weight loss. REX compatibilization of bioPE/KL blends with DCP has a positive effect on thermal stabilization at high temperatures, while the effect on the onset degradation temperature is not positive. REX with DCP increases the content of tertiary carbons which are prone to thermal decomposition. Anyway, since the difference between $T_{5\%}$ of neat bioPE (343.3 °C) and neat KL (138.1 °C) is so high, the first weight loss is attributable to lignin decomposition and, hence, the overall thermal stability of the bioPE/KL blends is compromised.[58] Similar results were reported by Krupa, et al.[62] They report the effect of DCP content on thermal properties of LLDPE/wax (80/20) blends. In fact, the onset degradation temperature for the uncompatibilized bled is 395.1 °C while the compatibilized blend by REX with 0.5 wt% DCP leads to a decrease in the onset degradation temperature down to 384.8 °C.

However, within the samples of bioPE/KL composites, the one with 1 phr DCP showed the highest $T_{5\%}$, which was 298.6 °C, this suggests that with high values of DCP is possible to improve T_{onset} temperatures in bioPE/KL composites. Furthermore, it can be seen the neat bioPE shows a noticeable weight loss after at 361 °C, and it is evident a weight loss delay in the blends of bioPE/KL and bioPE/KL/DCP. Since, it was observed a remarkable weight loss of bioPE/KL composite that starts from 429.7 °C, while in bioPE/KL/DCP composites this weight loss begins after 400 °C in

Table 5. Main thermal decomposition parameters of neat bioPE, uncompatibilized bioPE/KL blend, and bioPE/KL blend compatibilized by REX with varying DCP content in terms of onset degradation temperature ($T_{5\%}$), temperature of maximum degradation (T_{deg1}, T_{deg2}), and residual mass at 700 °C.

Sample	$T_{5\%}$ [°C]	T_{deg1} [°C]	T_{deg2} [°C]	Residual mass [%]
bioPE	343.3 ± 0.5 ^{a}	447.8 ± 1.0 ^{a}	–	0.4 ± 0.3 ^{a}
bioPE/KL	138.1 ± 0.9 ^{b}	282.4 ± 0.8 ^{b}/349.7 ± 0.6 ^{c}	481.2 ± 0.8 ^{a}	41.6 ± 0.5 ^{b}
bioPE/KL/0.25-DCP	309.7 ± 0.8 ^{c}	446.1 ± 1.2 ^{a}	481.7 ± 0.8 ^{a}	8.4 ± 0.8 ^{c}
bioPE/KL/0.50-DCP	284.3 ± 1.0 ^{d}	446.2 ± 0.6 ^{a}	483.3 ± 1.0 ^{a}	9.1 ± 1.3 ^{c}
bioPE/KL/0.75-DCP	232.3 ± 1.2 ^{e}	444.6 ± 1.1 ^{a}	484.8 ± 1.3 ^{a}	8.7 ± 0.9 ^{c}
bioPE/KL/1-DCP	258.2 ± 0.8 ^{f}	442.8 ± 1.4 ^{a}	491.4 ± 0.7 ^{a}	8.9 ± 1.1 ^{c}

$^{a-f}$Different letters in the same column indicate a significant difference among the samples ($p < 0.05$).

all cases, probably due to the effect of KL addition, into the composites, since KL has in its structure aromatic phenyl groups that are considered very stable due to the overlapping of p-orbitals, which allows complete delocalization of the π electrons, in addition, due to the presence of hydroxyl groups that contribute with the stability of these aromatic groups, which prevents its early break, that later only occur at high temperatures.[63,64] A similar trend is observed in the study performed by Gordobil et al.,[60] in that study blends with polylactic acid (PLA) and KL presented high thermal stability, regarding PLA sample. Lignin degradation is a complex process that takes place in a wide temperature range. As observed in Figure 5b, KL shows two main DTG peaks. First one located at 282.4 °C (first major degradation of lignin by pyrolysis) and a second peak at 349.7 °C related to a second major pyrolysis degradation of lignin by pyrolysis.[65,66] Furthermore, it is evident there are two main weight loss stages for all bioPE/KL blends. The first one is observed between 442.8 and 447.1 °C and is related to the maximum degradation rate of neat bioPE maximum located at 447.8 °C as shown in Figure 5b. The second peak appears above 480 °C in all bioPE/KL blends, which could be related to inter-unit linkages fragmentation, release of monomeric phenols into the vapor phase,[61,67] or release of aromatics and CO_2.[65] It is also important to bear in mind that the KL peak at 349.7 °C that corresponds to lignin is observed in all the composites with bioPE in Figure 5b. Finally, it was observed a residue at 700 °C for bioPE of 0.4 %, while for KL the value was 41.6%; similar values were also reported by Gordobil et al. and El Mansouri et al.[60,67]

Table 6. Dynamic mechanical analysis (DMTA) parameters of neat bioPE, uncompatibilized bioPE/KL blend, and REX-compatibilized bioPE/KL/DCP with increasing DCP content.

Sample	T_g [°C]	E' at −75 °C [MPa]	E' at 100 °C [MPa]
bioPE	−114.6 ± 0.8 ^{a}	1485.6 ± 7.3 ^{a}	118.2 ± 1.2 ^{a}
bioPE/KL	−118.9 ± 0.7 ^{a}	1823.6 ± 9.1 ^{b}	167.1 ± 1.4 ^{b}
bioPE/KL/0.25-DCP	−117.8 ± 1.0 ^{a}	1746.8 ± 8.6 ^{c}	175.5 ± 0.9 ^{b,c}
bioPE/KL/0.50-DCP	−117.2 ± 0.8 ^{a}	1956.1 ± 8.4 ^{d}	180.3 ± 1.1 ^{c}
bioPE/KL/0.75-DCP	−118.8 ± 1.3 ^{a}	1934.9 ± 6.9 ^{d,e}	168.9 ± 1.5 ^{c}
bioPE/KL/1-DCP	−120.2 ± 1.2 ^{a}	1928.4 ^{e}	157.1 ± 0.8 ^{d}

$^{a-e}$Different letters in the same column indicate a significant difference among the samples ($p < 0.05$).

3.4. Dynamic Mechanical Properties of bioPE/KL Blends

The dynamic mechanical behavior of neat bioPE and bioPE/KL blends was studied through the variation of storage modulus (E') and the dynamic damping factor (tan δ) as function of the temperature. In **Table 6** the different values can be observed. **Figure 6**a gathers the plots of the storage modulus (E') with increasing temperature. The typical dynamic mechanical thermal characterization of bioPE, reveals three peaks below the meting process, labeled as γ, β, and α relaxations that correspond to the different chain mobility related to a temperature increase. The γ-relaxation usually occurs in the temperature range from −150 to −100 °C, and it has been associated with the motion of the polymer chains in the amorphous phase.[68] According to Khonakdar et al.[58] and Munaro and Akcelrud,[69] this relaxation process is directly related to the glass transition temperature (T_g). The β-relaxation can be found at a temperature range close to or under room temperature. This is mainly associated with the segmental motions of the side chains in the non-crystalline region,[69] while the α-relaxation normally occurs at temperatures above room temperature, just approaching the melting temperature. The α-relaxation is associated with the crystalline region; in particular, it is related to the motion of chain folds at the surface of the crystalline lamellae.[68] As can be seen in Figure 6a, the γ- and β- relaxation can be clearly detected. The glass transition temperature for neat bioPE, was identified by following the peak maximum of the dynamic damping factor, at a peak maximum at −114.6 °C (Figure 6b). Above the T_g, E' values for bioPE decrease in a remarkable way since bioPE changes to an elastic-viscous behavior.[70] This happens when the temperature exceeds the α-relaxation of the biopolymer.[71] In particular, the storage modulus (E') of bioPE shows a value of 1485.6 MPa at −75 °C. Above the T_g, bioPE becomes more and more ductile (increase in the viscous component) and the corresponding E' values are remarkably reduced down to 118.2 MPa at 100 °C (more than 200 °C above its T_g). However, with the addition of KL to the polymeric matrix, it is observed a remarkable increase in E' at −75 °C with a value of 1823.6 MPa. It is important to remind that lignin has a T_g of about 160 °C, which makes it more elastic up to this temperature. On the other hand, REX compatibilization with 0.50, 0.75, and 1 phr of DCP leads to an increase in the storage modulus (E') to high values above 1900 MPa. This could be

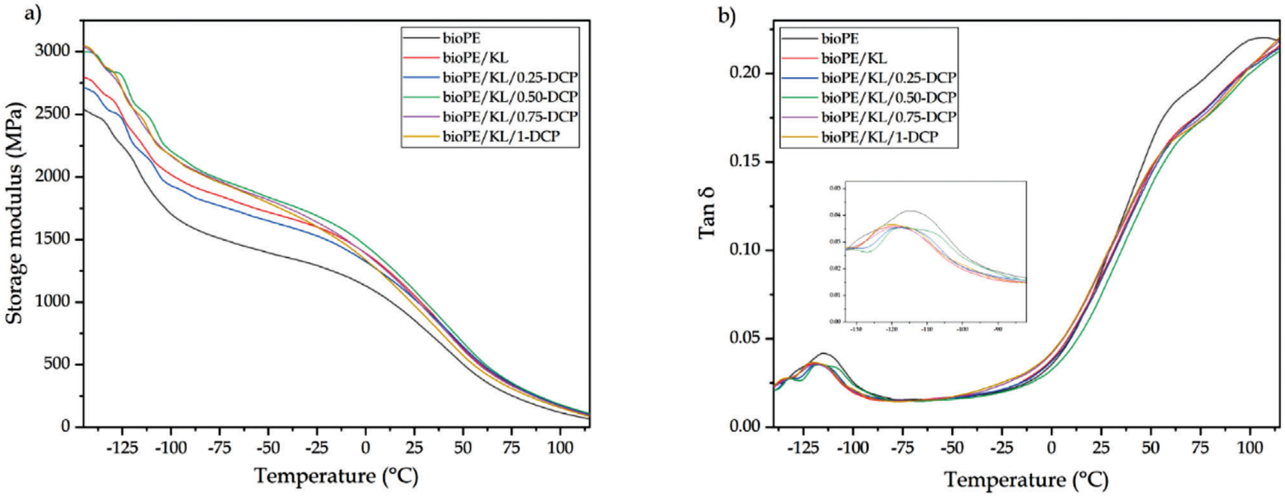

Figure 6. DMTA curves of the injection-molded pieces of neat bioPE, uncompatibilized bioPE/KL blend, and REX-compatibilized bioPE/KL with increasing DCP content, a) Storage modulus (E′) and b) Dynamic damping factor (tan δ).

explained due to the stiffening effect that causes the addition of KL and the REX process with DCP, which reduced the viscous constituent and restrict the polymer mobility, giving rise to the elastic component.[72] This corroborates that REX with DCP provides somewhat compatibilization between bioPE and KL.[73]

Figure 6b, shows the evolution of the dynamic damping factor (tan δ) of neat bioPE and bioPE/KL blends. The glass transition temperature (T_g) of the different samples was identified as the peak of tan δ and ranged between −108 to −120 °C (Figure 6b). It is also worth noting that uncompatibilized bioPE/KL blends, and specially REX-compatibilized bioPE/KL blends with DCP offer lower tan δ values, which could indicate that these materials show a more elastic response, and therefore, they have the potential to store the applied load rather than to dissipate/loss it.[71]

3.5. Wettability of bioPE/KL Blends

In general, surfaces with a water-contact angle between 0° to 30° can be considered as hydrophilic materials, on the other hand, a value above 90° indicates hydrophobic materials.[74] **Figure 7** clearly indicates the angles obtained by the different samples. In this regard, neat bioPE is a highly hydrophobic polymer due to its nonpolar structure, which leads to a water-contact angle (θ_w) of 95.1°.[53] The addition of KL causes a decrease in the hydrophobicity of bioPE, as expected, due to the polar groups contained in lignin. Hence, the water-contact angle decreases to 85°, which is still high. Despite lignin has polar groups, it shows low hydrophilicity.[75] A similar behavior was reported by Sousa Junior et al.[76] in which PP showed a water-contact angle of 107.22°, and then with the addition of acid or alkali KL, the water-contact angle decreased to values between 91° and 98°, depending on the lignin content. REX with increasing DCP content, leads to a decrease in the water-contact angle, reaching a value of 71.4° for the REX-compatibilized blend with 1 phr DCP. It seems REX provides more polarity to the surface as a consequence of the reaction products obtained after the decomposition of DCP in the extruder and the subsequent free radical formation which could lead to branching, crosslinking, among others.[77] These results agree with those reported by Ararat et al.[78] in which the effect of DCP on surface wetting properties of a blend of LDPE and a maleinized hyperbranched polyester is studied. They concluded that the water-contact angle is lower for increasing the DCP content in the reactive compatibilization process. In fact, the initial water-contact angle of neat LDPE was 96°, and was decreased to 78°, 62°, and 54°, with reactive compatibilization using 0.5, 1.0, and 1.5 wt% DCP, respectively.

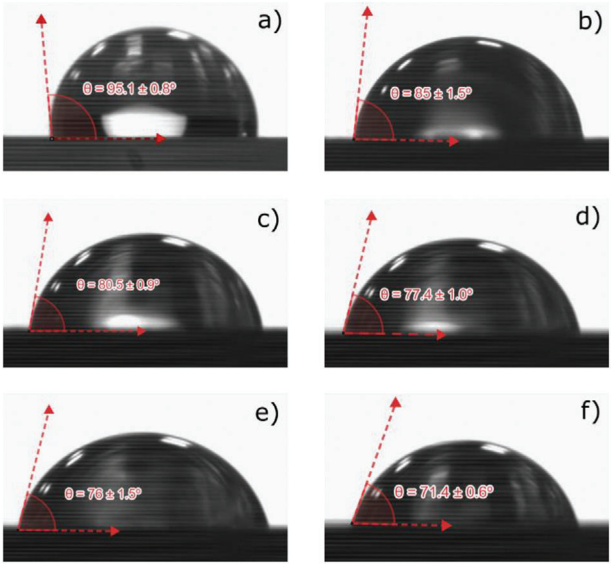

Figure 7. Wettability through contact angle measurements of a) neat bioPE, b) bioPE/KL, c) bioPE/KL/0.25-DCP, d) bioPE/KL/0.50-DCP, e) bioPE/KL/0.75-DCP, and f) bioPE/KL/1-DCP.

According to Bova et al.,[34] the use of DCP remarkably improves mechanical strength of acrylonitrile-butadiene rubber with different lignins, thus showing the efficiency of DCP as reactive compatibilizer in these blends. As it has been previously shown in FESEM characterization, as the DCP loading increases, the dispersed lignin domain phase is clearly lowered which, in turn, increases the surface area of lignin. Furthermore, it is important to bear in mind that KL usually contains some salt impurities. Gordobil et al.[79] reported the presence of some residual carbohydrates, ashes, and sulfur in KL. These impurities, together with the finer KL domains contribute to the observed increased hydrophilicity with increasing DCP.

4. Conclusions

bioPE and KL blends were successfully compatibilized by REX with an organic peroxide, namely DCP in the 0–1 phr range. The tensile tests indicated a remarkable improvement in mechanical properties after the REX process with increasing DCP content. In particular, REX with 1 phr DCP led to a bioPE/KL blend with an increase in elongation at break of about 300% with regard to the uncompatibilized blend. Similar tendency was observed for the impact strength, thus giving evidence that REX with DCP is a feasible, easy, and cost-effective process to provide some compatibility between bioPE and KL. FESEM revealed a phase separation (drop-like) in uncompatibilized bioPE/KL blends, with lignin aggregates. The use of REX with increasing DCP content, prevents aggregate formation and the lignin size domain is remarkably reduced, thus indicating a better particle dispersion. DSC revealed a slight decrease in the degree of crystallinity of bioPE in REX-compatibilized bioPE/KL blends due to formation of less perfect crystals resulting from the branched or crosslinked species obtained during the REX process which provide more polar properties to the surfaces, as corroborated by a decrease in the water-contact angle (θ_w) with increasing DCP content in the REX process. Despite lignin is less thermally stable than bioPE, the overall thermal stability of these blends is not compromised in terms of processing temperatures. Moreover, these blends show a dark brown color that could be interesting for use of these blends as a WPC. Therefore, the results obtained in this work offer the possibility to use a natural polymer (KL) in a bioPE matrix to obtain a material with overall balanced properties using REX with DCP.

Acknowledgements

S.R.-L. is a recipient of a Santiago Grisolía grant from Generalitat Valenciana (GVA) (GRISOLIAP/2019/132). D.L. thanks Universitat Politècnica de València (UPV) for the grant received through the PAID-01-18 program. J.I.-M. thanks the Spanish Ministry of Science, Innovation and Universities for his FPU grant (FPU19/01759). Microscopy services at UPV are acknowledged for their help in using and collecting FESEM images.

Conflict of Interest

The authors declare no conflict of interest.

Data Availability Statement

Research data are not shared.

Keywords

bio-polyethylene, blends, dicumyl peroxide, kraft lignin, reactive compatibilization

Received: March 24, 2021
Revised: May 3, 2021

---

[1] M. A. Abdelwahab, S. Taylor, M. Misra, A. K. Mohanty, *Macromol. Mater. Eng.* **2015**, *300*, 299.
[2] A. Tejado, C. Pena, J. Labidi, J. Echeverria, I. Mondragon, *Bioresour. Technol.* **2007**, *98*, 1655.
[3] S. Huang, N. Mahmood, M. Tymchyshyn, Z. Yuan, C. C. Xu, *Bioresour. Technol.* **2014**, *171*, 95.
[4] J. Mei, W. Liu, J. Huang, X. Qiu, *Macromol. Mater. Eng.* **2019**, *304*, 1800689.
[5] A. Duval, M. Lawoko, *React. Funct. Polym.* **2014**, *85*, 78.
[6] H. Li, Y. Deng, B. Liu, Y. Ren, J. Liang, Y. Qian, X. Qiu, C. Li, D. Zheng, *ACS Sustainable Chem. Eng.* **2016**, *4*, 1946.
[7] Q. Tang, Y. Qian, D. Yang, X. Qiu, Y. Qin, M. Zhou, *Polymers* **2020**, *12*, 2471.
[8] N. Jamil, P. Kumar, R. Batool, In *Soil Microenvironment for Bioremediation and Polymer Production*, Wiley, New York **2020**.
[9] H. Chen, X. Qu, N. Liu, S. Wang, X. Chen, S. Liu, *Chem. Eng. Res. Des.* **2018**, *139*, 248.
[10] A. Zerpa, L. Pakzad, P. Fatehi, *ACS Omega* **2018**, *3*, 8233.
[11] Y. Meng, J. Lu, Y. Cheng, Q. Li, H. Wang, *Int. J. Biol. Macromol.* **2019**, *135*, 1006.
[12] H. Jeong, J. Park, S. Kim, J. Lee, J. W. Cho, *Fibers Polym.* **2012**, *13*, 1310.
[13] S. C. Lee, T. M. T. Tran, J. W. Choi, K. Won, *Int. J. Biol. Macromol.* **2019**, *122*, 549.
[14] H. Sadeghifar, D. S. Argyropoulos, *ACS Sustainable Chem. Eng.* **2016**, *4*, 5160.
[15] X. Tian, Z. Fang, R. L. Smith, Z. Wu, M. Liu, In *Production of Biofuels and Chemicals from Lignin*, Springer, New York **2016**, p. 3.
[16] O. A. T. Dias, D. R. Negrão, D. F. C. Gonçalves, I. Cesarino, A. L. Leão, *Mol. Cryst. Liq. Cryst.* **2017**, *655*, 204.
[17] M. Wei, L. Fan, J. Huang, Y. Chen, *Macromol. Mater. Eng.* **2006**, *291*, 524.
[18] L. Dehne, C. V. Babarro, B. Saake, K. U. Schwarz, *Ind. Crops Prod.* **2016**, *86*, 320.
[19] O. Dias, D. Negrão, R. Silva, C. Funari, I. Cesarino, A. Leao, *Mol. Cryst. Liq. Cryst.* **2016**, *628*, 72.
[20] G. Cazacu, M. C. Pascu, L. Profire, A. Kowarski, M. Mihaes, C. Vasile, *Ind. Crops Prod.* **2004**, *20*, 261.
[21] S. Kumar, A. Mohanty, L. Erickson, M. Misra, *J. Biobased Mater. Bioenergy* **2009**, *3*, 1.
[22] L. Hu, T. Stevanovic, D. Rodrigue, *J. Appl. Polym. Sci.* **2014**, *131*, 41040.
[23] G. M. Farias, P. Agrawal, R. B. Hanken, J. P. de Araújo, A. D. de Oliveira, T. J. de Mélo, *J. Therm. Anal. Calorim.* **2021**, 1.
[24] I. Tsiropoulos, A. P. Faaij, L. Lundquist, U. Schenker, J. F. Briois, M. K. Patel, *J. Cleaner Prod.* **2015**, *90*, 114.
[25] D. Garcia-Garcia, A. Carbonell-Verdu, A. Jordá-Vilaplana, R. Balart, D. Garcia-Sanoguera, *J. Appl. Polym. Sci.* **2016**, *133*.
[26] A. Tribot, G. Amer, M. A. Alio, H. de Baynast, C. Delattre, A. Pons, J.-D. Mathias, J.-M. Callois, C. Vial, P. Michaud, *Eur. Polym. J.* **2019**, *112*, 228.
[27] M. Przybysz, M. Marć, M. Klein, M. R. Saeb, K. Formela, *Polym. Test.* **2018**, *67*, 513.
[28] W. Brostow, T. Datashvili, K. P. Hackenberg, *Polym. Compos.* **2010**, *31*, 1678.
[29] R. Muthuraj, M. Misra, A. K. Mohanty, *J. Appl. Polym. Sci.* **2018**, *135*, 45726.
[30] R. Sailaja, M. Deepthi, *Mater. Des.* **2010**, *31*, 4369.

[31] G. Toriz, F. Denes, R. Young, *Polym. Compos.* **2002**, *23*, 806.
[32] M. Ghozali, E. Triwulandari, A. Haryono, E. Yuanita, In *IOP Conference Series: Materials Science and Engineering*, IOP Publishing, Bristol, UK **2017**, p. 223/012022.
[33] R. Anbarasan, O. Babot, B. Maillard, *J. Appl. Polym. Sci.* **2004**, *93*, 75.
[34] T. Bova, C. D. Tran, M. Y. Balakshin, J. Chen, E. A. Capanema, A. K. Naskar, *Green Chem.* **2016**, *18*, 5423.
[35] D. Garcia-Garcia, E. Rayón, A. Carbonell-Verdu, J. López-Martínez, R. Balart, *Eur. Polym. J.* **2017**, *86*, 41.
[36] A. Zattera, O. Bianchi, R. d. Oliveira, L. Canto, C. Ferreira, M. Zeni, *Prog. Rubber, Plast. Recycl. Technol.* **2006**, *22*, 69.
[37] P. Ma, X. Cai, Y. Zhang, S. Wang, W. Dong, M. Chen, P. Lemstra, *Polym. Degrad. Stab.* **2014**, *102*, 145.
[38] E. Ahmad, A. Luyt, *Composites, Part A* **2012**, *43*, 703.
[39] J. Huang, W. Liu, X. Qiu, *ACS Sustainable Chem. Eng.* **2019**, *7*, 6550.
[40] J. F. Kadla, S. Kubo, *Macromolecules* **2003**, *36*, 7803.
[41] V. K. Thakur, M. K. Thakur, P. Raghavan, M. R. Kessler, *ACS Sustainable Chem. Eng.* **2014**, *2*, 1072.
[42] F. Dominici, D. García García, V. Fombuena, F. Luzi, D. Puglia, L. Torre, R. Balart, *Molecules* **2019**, *24*, 3113.
[43] X. Qiu, J. Yu, D. Yang, J. Wang, W. Mo, Y. Qian, *ACS Sustainable Chem. Eng.* **2018**, *6*, 1055.
[44] K. Krisdianto, *Indonesian Journal of Forestry Research* **2007**, *4*, 83.
[45] L. Quiles-Carrillo, N. Montanes, A. Jorda-Vilaplana, R. Balart, S. Torres-Giner, *J. Appl. Polym. Sci.* **2019**, *136*, 47396.
[46] F. Chen, W. Liu, S. I. Seyed Shahabadi, J. Xu, X. Lu, *ACS Sustainable Chem. Eng.* **2016**, *4*, 4997.
[47] X. He, F. Luzi, X. Hao, W. Yang, L. Torre, Z. Xiao, Y. Xie, D. Puglia, *Int. J. Biol. Macromol.* **2019**, *127*, 665.
[48] W. Zhao, L.-P. Xiao, G. Song, R.-C. Sun, L. He, S. Singh, B. A. Simmons, G. Cheng, *Green Chem.* **2017**, *19*, 3272.
[49] B. Bozsódi, V. Romhányi, P. Pataki, D. Kun, K. Renner, B. Pukánszky, *Mater. Des.* **2016**, *103*, 32.
[50] F. X. Espinach, E. Espinosa, R. Reixach, A. Rodríguez, P. Mutjé, Q. Tarrés, *Polymers* **2020**, *12*, 2206.
[51] J. M. Ferri, D. Garcia-Garcia, E. Rayón, M. D. Samper, R. Balart, *Polymers* **2020**, *12*, 1344.
[52] M. A. Abdelwahab, M. Misra, A. K. Mohanty, *Ind. Crops Prod.* **2019**, *132*, 497.
[53] J. Sameni, S. A. Jaffer, M. Sain, *Composites, Part A* **2018**, *115*, 104.
[54] B. Fei, C. Chen, S. Chen, S. Peng, Y. Zhuang, Y. An, L. Dong, *Polym. Int.* **2004**, *53*, 937.
[55] P. Ma, D. G. Hristova-Bogaerds, P. J. Lemstra, Y. Zhang, S. Wang, *Macromol. Mater. Eng.* **2012**, *297*, 402.
[56] C. Mao, C. X. Liang, Y. Q. Mao, L. Li, X. M. Hou, J. Shen, *Colloids Surf., B* **2009**, *74*, 362.
[57] V. Katiyar, *J. Therm. Anal. Calorim.* **2019**, *138*, 195.
[58] H. Khonakdar, J. Morshedian, U. Wagenknecht, S. Jafari, *Polymer* **2003**, *44*, 4301.
[59] C. Huang, J. He, R. Narron, Y. Wang, Q. Yong, *ACS Sustainable Chem. Eng.* **2017**, *5*, 11770.
[60] O. Gordobil, R. Delucis, I. Egüés, J. Labidi, *Ind. Crops Prod.* **2015**, *72*, 46.
[61] F. Bertini, M. Canetti, A. Cacciamani, G. Elegir, M. Orlandi, L. Zoia, *Polym. Degrad. Stab.* **2012**, *97*, 1979.
[62] I. Krupa, A. Luyt, *Polym. Degrad. Stab.* **2000**, *70*, 111.
[63] A. A. Morandim-Giannetti, J. A. M. Agnelli, B. Z. Lanças, R. Magnabosco, S. A. Casarin, S. H. Bettini, *Carbohydr. Polym.* **2012**, *87*, 2563.
[64] L. R. Chiappero, S. S. Bartolomei, D. A. Estenoz, E. A. Moura, V. V. Nicolau, *J. Polym. Environ.* **2021**, *29*, 450.
[65] M. Zhang, F. L. Resende, A. Moutsoglou, D. E. Raynie, *J. Anal. Appl. Pyrolysis* **2012**, *98*, 65.
[66] D. Shen, S. Gu, K. Luo, S. Wang, M. Fang, *Bioresour. Technol.* **2010**, *101*, 6136.
[67] N.-E. El Mansouri, Q., Yuan, F., Huang, *BioResources* **2011**, *6*, 2492.
[68] R. Sirotkin, N. Brooks, *Polymer* **2001**, *42*, 9801.
[69] M. Munaro, L. Akcelrud, *J. Polym. Res.* **2008**, *15*, 83.
[70] S. Torres-Giner, N. Montanes, O. Fenollar, D. García-Sanoguera, R. Balart, *Mater. Des.* **2016**, *108*, 648.
[71] J. Ivorra-Martinez, L. Quiles-Carrillo, T. Boronat, S. Torres-Giner, J. A. Covas, *Polymers* **2020**, *12*, 1389.
[72] H. Kargarzadeh, A. Galeski, A. Pawlak, *Polymer* **2020**, *203*, 122748.
[73] Á. Agüero, D. Garcia-Sanoguera, D. Lascano, S. Rojas-Lema, J. Ivorra-Martinez, O. Fenollar, S. Torres-Giner, *Polymers* **2020**, *12*, 821.
[74] A. Jordá-Vilaplana, V. Fombuena, D. García-García, M. Samper, L. Sánchez-Nácher, *Eur. Polym. J.* **2014**, *58*, 23.
[75] K. Kaewtatip, J. Thongmee, *Mater. Des.* **2013**, *49*, 701.
[76] R. R. D. Sousa Junior, J. R. Gouveia, A. M. Nacas, L. B. Tavares, N. M. Ito, E. N. D. Moura, F. A. Gaia, R. F. Pereira, D. J. D. Santos, *Mater. Res.* **2019**, *22*, 1.
[77] C. B. Luna, D. D. Siqueira, E. M. Araújo, R. M. Wellen, T. Jeferson Alves de Mélo, *J. Vinyl Addit. Technol.* **2020**, *27*, 308.
[78] C. Ararat, E. Murillo, In *Journal of Physics: Conference Series*, IOP Publishing, Bristol, UK **2019**, p. 1386/012069.
[79] O. Gordobil, R. Moriana, L. Zhang, J. Labidi, O. Sevastyanova, *Ind. Crops Prod.* **2016**, *83*, 155.